

A MEASUREMENT OF THE η RADIATIVE WIDTH $\Gamma_{\eta \rightarrow \gamma\gamma}$

JADE Collaboration

W. BARTEL, L. BECKER, D. CORDS¹, R. FELST, D. HAIDT, H. JUNGE², G. KNIES,
H. KREHBIEL, P. LAURIKAINEN³, R. MEINKE, B. NAROSKA, J. OLSSON, D. SCHMIDT⁴,
P. STEFFEN⁵

Deutsches Elektronen-Synchrotron DESY, Hamburg, Germany

G. DIETRICH, J. HAGEMANN, G. HEINZELMANN, H. KADO, K. KAWAGOE⁶,
C. KLEINWORT, M. KUHLN, K. MEIER⁵, A. PETERSEN¹, R. RAMCKE,
U. SCHNEEKLOTH, G. WEBER

II Institut für Experimentalphysik der Universität Hamburg, Hamburg, Germany

K. AMBRUS, S. BETHKE, A. DIECKMANN, E. ELSN, J. HEINTZE, K.-H. HELLENBRAND,
S. KOMAMIYA, J. VON KROGH, P. LENNERT, H. MATSUMURA, H. RIESEBERG,
J. SPITZER, A. WAGNER

Physikalisches Institut der Universität Heidelberg, Heidelberg, Germany

C. BOWDERY, A. FINCH, F. FOSTER, G. HUGHES, T. NOZAKI⁷, J. NYE

University of Lancaster, Lancaster, England

J. ALLISON, J. BAINES, A.H. BALL⁸, R.J. BARLOW, J. CHRIN, I.P. DUERDOTH,
T. GREENSHAW, P. HILL, F.K. LOEBINGER, A.A. MACBETH, H. McCANN, H.E. MILLS,
P.G. MURPHY, K. STEPHENS, P. WARMING

University of Manchester, Manchester, England

R.G. GLASSER, B. SECHI-ZORN⁹, J.A.J. SKARD, S.R. WAGNER, G.T. ZORN

University of Maryland, College Park, MD, USA

S.L. CARTWRIGHT, D. CLARKE, R. MARSHALL, R.P. MIDDLETON, J.B. WHITTAKER

Rutherford Appleton Laboratory, Chilton, England

T. KAWAMOTO, T. KOBAYASHI, T. MASHIMO, M. MINOWA, H. TAKEDA, T. TAKESHITA
and S. YAMADA

International Center for Elementary Particle Physics, University of Tokyo, Tokyo, Japan

Received 15 April 1985

*We wish to dedicate this letter to our friend Bice Sechi-Zorn
who contributed so much to this work.*

The radiative width of the η meson has been measured at PETRA in photon-photon collisions. The resulting value is $\Gamma_{\eta \rightarrow \gamma\gamma} = 0.53 \pm 0.04 \pm 0.04$ keV.

For footnotes see next page.

The decay widths into two photons of the mesons π^0 , $\eta(548)$ and $\eta(958)$ are of considerable interest. They can be related to the well-known questions of quark content and octet-singlet mixing in the pseudoscalar nonet [1], as well as to the fundamental question of fractional or integer quark charges [2]. They are also of importance for the discussion of a gluonic admixture in the pseudoscalar mesons and their relation to the pseudoscalar glueball candidate, $\omega(1440)^{\#1}$.

The radiative width $\Gamma_{\pi^0 \rightarrow \gamma\gamma}$ is very accurately determined [4] and many measurements of $\Gamma_{\eta' \rightarrow \gamma\gamma}$ have recently been presented [5-9]. Relatively few measurements of $\Gamma_{\eta \rightarrow \gamma\gamma}$ have been made, however. The early measurements [10] which used the Primakoff effect [11] in photoproduction differ considerably from each other, and a recent measurement [12] which was obtained from $\gamma\gamma$ production of η in e^+e^- collisions, does not allow a definite conclusion.

We present in this letter a new measurement of $\Gamma_{\eta \rightarrow \gamma\gamma}$, where the η mesons were produced via the reaction

$$e^+e^- \rightarrow e^+e^-\eta, \quad \eta \rightarrow \gamma\gamma. \quad (1)$$

The e^+ and e^- beam particles were scattered at small angles and were not detected. Thus the only detected particles from this reaction were the two photons from the η decay.

The experiment was performed at the e^+e^- storage ring PETRA, at a beam energy of 17.3 GeV. The detector used was JADE, a general purpose, large solid angle, charged particle and photon detector operating with a magnetic field of 0.48 tesla. Detailed descriptions of JADE appear in ref. [13]. In this experiment, photon detection was of particular importance. Photons were detected by an array of 2712 lead-glass

counters located outside of the central jet chamber and the magnet coil. They furnish complete azimuthal (ϕ) coverage over a θ range given by $|\cos \theta| < 0.82$ for the central barrel and $0.89 < |\cos \theta| < 0.97$ for the end caps, where θ is measured relative to the e^+ beam. The barrel consists of 30 rings, each with 84 counters. A single counter subtends $\sim 4^\circ$ in azimuth.

A special trigger was set up for the detection of reaction (1) and other exclusive $\gamma\gamma$ reactions. The lead-glass barrel counters were grouped in azimuth, ϕ , into seven sectors (henceforth called septants) and the linear analogue sum of the pulse-heights of the 360 counters in each septant was used to generate a septant signal. For the trigger, a coincidence was required between two septants, separated by at least two other septants, with all time-of-flight (TOF) scintillation counters in anticoincidence. A maximum of three septant signals was allowed. The signal threshold for triggering was at two levels, low threshold (run I) and high threshold (run II). Fig. 1 shows the linear sum trigger signal efficiency as a function of measured energy in septants for the low and the high thresholds. These curves were obtained from event samples selected using other, independent triggers. The chosen thresholds are below the typical deposited energy of 0.15-0.30 GeV for photons from reaction (1).

Events were required to satisfy the criteria described below:

- (i) Two and only two photons should be detected in the lead-glass barrel and no other photons in the endcaps. This selection used a cluster algorithm which chose acceptable photon signals. The detection thresh-

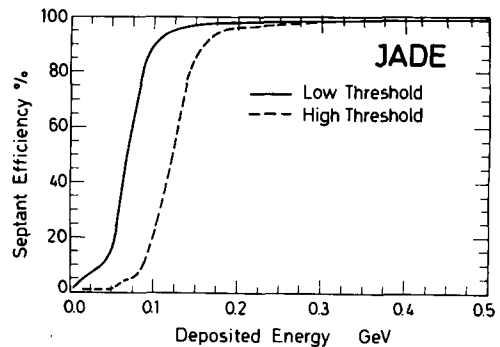


Fig. 1. Trigger signal efficiency of lead-glass counter septants as a function of detected energy, for low threshold operation (continuous curve) and for high threshold operation (dashed curve).

¹ Present address: SLAC, Stanford, CA, USA.
² Present address: Krupp Atlas Elektronik, Bremen, Germany.
³ University of Helsinki, Helsinki, Finland.
⁴ Universität-Gesamthochschule Wuppertal, Wuppertal, Germany.
⁵ Present address: CERN, Geneva, Switzerland.
⁶ Deutscher Akademischer Austauschdienst (DAAD) Fellow.
⁷ Present address: KEK, Ibaraki, Japan.
⁸ Present address: University of Maryland, College Park, MD, USA.
⁹ Deceased.

^{#1} An extensive list of references can be found in reference [38] of ref. [3].

olds were 0.045 GeV for a single counter and 0.060 GeV for a cluster of adjacent counters. These detection thresholds were determined by the electronics readout threshold, which was 0.025–0.030 GeV for each counter.

(ii) No charged particles should be detected in the jet chamber by the pattern recognition program.

(iii) Events with penetrating cosmic ray muons, detected in the external muon chambers covering 92% of the total solid angle, were rejected.

(iv) The remaining cosmic ray muons which traversed the lead-glass array but not the jet chamber were rejected by excluding events in which both photons had $|\cos \theta| > 0.68$ ^{‡2} and where $\cos \theta_1 \cdot \cos \theta_2 > 0$.

(v) The acoplanarity angle $\Delta\phi$, defined as the smallest angle between the planes formed by each photon position and the beam line, was required to be smaller than 20° . This restricted the event sample to an angular region favoured by reaction (1), as shown below.

(vi) Both photons in an event were required to have energies above 0.140 GeV and below 3 GeV. The latter restriction was imposed in order to exclude events from the QED reaction $e^+e^- \rightarrow \gamma\gamma$.

(vii) All remaining events were visually inspected and events were eliminated if evidence of any charged particle track was seen in the jet chamber.

(viii) The observed transverse momentum of the $\gamma\gamma$ system, $|p_\perp|$, relative to the e^+e^- beam directions, was required to be smaller than 0.120 GeV/c. This cut serves to decrease background from beam–gas reactions as well as from other $\gamma\gamma$ reactions with additional, undetected final-state particles. It also limits the momentum transfer (q^2) of the virtual photons in reaction (1) to $|q^2| < 0.04$ (GeV/c)², with a mean $\langle q^2 \rangle \cong -2 \times 10^{-4}$ (GeV/c)². The p_\perp^2 distribution for the events of run I and II summed together is shown in fig. 2. The p_\perp^2 limit is indicated by an arrow.

For the purpose of beam–gas background estimation, a third data sample, obtained in a run with the low threshold condition with separated e^+e^- beams (run III), was subjected to the same selection criteria. The numbers of events remaining after all of the above restrictions for each of the samples are listed in table 1.

^{‡2} Here, as well as in the invariant mass calculation, the event vertex is taken to be the center of the detector, which coincides closely with the average e^+e^- collision point.

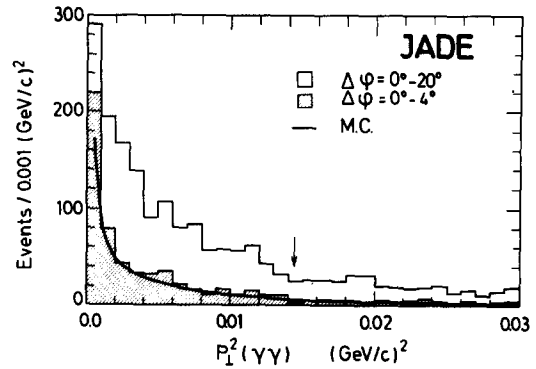


Fig. 2. The distribution of p_\perp^2 of the $\gamma\gamma$ system relative to the beam, for all events of runs I and II passing the selection criteria (i)–(vii). The shaded histogram shows the same distribution with the additional requirement on acoplanarity: $\Delta\phi = 0^\circ - 4^\circ$. The continuous curve shows the Monte Carlo simulation result (see text).

The $\gamma\gamma$ invariant mass spectrum of the 1473 selected events from run I and II is shown as a solid line histogram in fig. 3. The distribution shows a clear peak in the η mass region. In addition to reaction (1), also other exclusive $\gamma\gamma$ reactions may contribute to this mass spectrum. The following reactions were considered:

$$\begin{aligned}
 e^+e^- &\rightarrow e^+e^-\eta'; & \eta' &\rightarrow \pi^+\pi^-\eta, \pi^0\pi^0\eta, \gamma\gamma; \\
 & & \eta &\rightarrow \gamma\gamma, \\
 e^+e^- &\rightarrow e^+e^-f; & f &\rightarrow \pi^0\pi^0; \\
 e^+e^- &\rightarrow e^+e^-A_2; & A_2 &\rightarrow \eta\pi^0; \\
 & & \eta &\rightarrow \gamma\gamma.
 \end{aligned} \tag{2}$$

With the exception of the decay $\eta' \rightarrow \gamma\gamma$, events from reactions (2) are incompletely measured and constitute a background to reaction (1). Also beam–gas reactions contribute. The mass spectrum of the 30 events in the separated beam data sample is also shown in fig. 3 (solid histogram). These events contribute only in the mass region below 0.8 GeV/c².

In order to evaluate the contribution of reaction (1) to the mass spectrum of fig. 3 we will use the acoplanarity, $\Delta\phi$, for events with $\gamma\gamma$ invariant mass < 0.8 GeV/c² (the maximum mass value found in the Monte Carlo simulation of reaction (1)). The acoplanarity distribution is shown in fig. 4a with the events of runs I and II summed together. A prominent peak at $\Delta\phi \sim$

Table 1
Determination of $\Gamma_{\eta \rightarrow \gamma\gamma}$.

	Trigger condition, data sample		
	Low threshold		High threshold
	run I	run III separated beams	run II
integrated luminosity (pb^{-1})	17.1	—	14.6
selected event sample	888	30	585
selected event sample with $m(\gamma\gamma) < 0.8 \text{ GeV}/c^2$			
$\Delta\phi = 0^\circ - 4^\circ$	271	2	224
$\Delta\phi = 4^\circ - 20^\circ$	562	28	316
Monte Carlo event sample ^{a)} (reaction (1))			
$\Delta\phi = 0^\circ - 4^\circ$	3996	—	3100
$\Delta\phi = 4^\circ - 20^\circ$	1654	—	1501
Monte Carlo event sample with $m(\gamma\gamma) < 0.8 \text{ GeV}/c^2$ (reactions (2), normalized)			
$\Delta\phi = 0^\circ - 4^\circ$	3.4	—	2.9
$\Delta\phi = 4^\circ - 20^\circ$	7.8	—	6.8
beam-gas background subtraction factor B	15.7 \pm 3.2	—	7.5 \pm 1.6
selected event sample, with $m(\gamma\gamma) < 0.8 \text{ GeV}/c^2$, background subtracted			
$\Delta\phi = 0^\circ - 4^\circ$	236.2 \pm 29.3	—	206.1 \pm 19.2
detection efficiency ^{b)} (%)	2.62 \pm 0.05	—	2.46 \pm 0.05
$\sigma(e^+e^- \rightarrow e^+e^-\eta)$ ^{b)} (nb)	1.35 \pm 0.17	—	1.48 \pm 0.14
$\Gamma_{\eta \rightarrow \gamma\gamma}$ (keV)	0.506 \pm 0.064	—	0.554 \pm 0.054
$\Gamma_{\eta \rightarrow \gamma\gamma}$, weighted average (keV)		0.534 \pm 0.041	

^{a)} There are no events with $m(\gamma\gamma) > 0.8 \text{ GeV}/c^2$.

^{b)} These values are calculated for electron scattering angles $< 35 \text{ mrad}$.

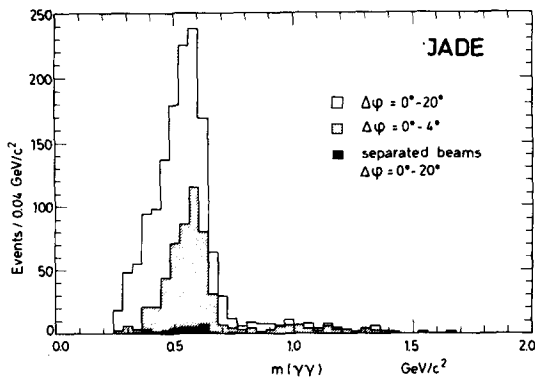


Fig. 3. Invariant $\gamma\gamma$ mass distribution for all events of runs I and II passing the selection criteria (i)–(viii). The shaded histogram shows the mass spectrum with the additional requirement on acoplanarity: $\Delta\phi = 0^\circ - 4^\circ$. The solid histogram shows the mass distribution for separated beam events (run III) passing selection criteria (i)–(viii).

0° is noted in the data ^{#3}. A similar peak is also seen in the Monte Carlo simulation of reaction (1), shown as a shaded histogram in fig. 4b. This peak, however, is not seen in the separated beam data in fig. 4c (solid histogram), nor in the distribution for events excluded in the visual scan shown in fig. 4d, nor in the normalized background distribution ^{#4} of reactions (2) in fig. 4e. This peak is interpreted as evidence for

^{#3} The regular structure seen in this distribution reflects the lead-glass counter size of $\sim 4^\circ$ in azimuth ϕ .

^{#4} For the normalization, the average values for $\Gamma_{\eta' \rightarrow \gamma\gamma}$, $\Gamma_{f \rightarrow \gamma\gamma}$ and $\Gamma_{A_2 \rightarrow \gamma\gamma}$ of ref. [14] were used.

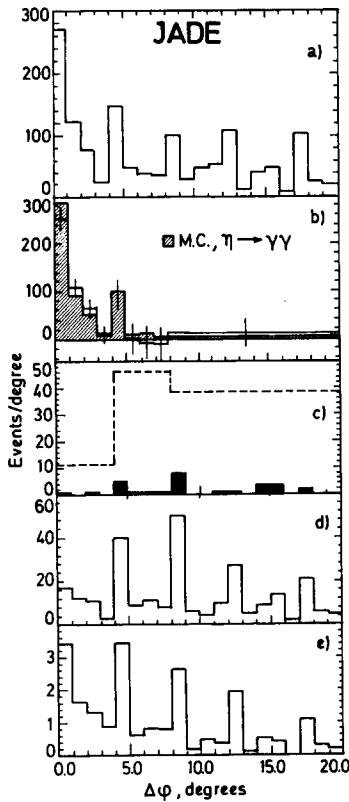


Fig. 4. The distribution of acoplanarity angle $\Delta\phi$ for events with $m(\gamma\gamma) < 0.8 \text{ GeV}/c^2$, selected with criteria (i)–(viii): (a) for events of runs I and II, (b) for fully background subtracted run I and II data with the shaded histogram showing the normalized Monte Carlo simulation result, (c) for events of run III with separated beams (solid histogram) and for the normalized distribution calculated with the factor B (dashed line histogram, see text), (d) for events excluded in the visual scan, and (e) for the normalized background from other beam–beam interactions (reaction (2)) from Monte Carlo simulation.

exclusive production of a state decaying into two photons, as in reaction (1).

To obtain a background subtracted η signal, the $\Delta\phi$ distribution was divided into two regions: 0° – 4° where the η signal is dominant over background, and 4° – 20° where the background is dominant. The effect of the $\Delta\phi = 0^\circ$ – 4° interval selection in reducing background can be seen in fig. 2, where the corresponding p_{\perp}^2 distribution for the $\gamma\gamma$ system is shown as a shaded histogram. Compared to the p_{\perp}^2 distribution in the 0° – 20° interval, it is noticeably more peaked towards low values, as expected for events of reaction (1). The mass distribution of all events in the 0° – 4° interval is given by the shaded histogram in fig. 3. It shows a narrower and more centered η signal than that seen in the mass distribution for the 0° – 20° interval. The numbers of events in the 0° – 4° and 4° – 20° intervals are given in table 1 for the data samples of runs I, II, and III, together with the corresponding numbers for the Monte Carlo simulations of reaction (1) and reactions (2).

We now evaluate the number of beam–gas events to be subtracted as background in the interval 0° – 4° . The magnitude of this background is estimated using the separated beam data, normalized to the colliding beam data by the relation

$$\frac{N_d(0^\circ-4^\circ) - BN_{bg}(0^\circ-4^\circ)}{N_{MC}(0^\circ-4^\circ)} = \frac{N_d(4^\circ-20^\circ) - BN_{bg}(4^\circ-20^\circ)}{N_{MC}(4^\circ-20^\circ)} \quad (3)$$

Here the values in parentheses specify the $\Delta\phi$ angular region covered. N_d is the number of events in the given $\Delta\phi$ region for the colliding beam data sample (fig. 4a), with the normalized contributions of reactions (2) (fig. 4e) subtracted. N_{bg} and N_{MC} are the numbers of events for the beam–gas events from the separated beam data (fig. 4c) and for the Monte Carlo simulation of reaction (1), respectively. B is the required normalization factor. The values of B determined from relation (3) for run I and II are given in table 1 ^{#5}. The

^{#5} The same separated beam data (taken with run I trigger conditions) were used to determine the background subtraction for both run I and II, i.e. we assume that the shape of the $\Delta\phi$ distribution of beam–gas events does not change from run I to run II. This is a reasonable, although unverifiable, assumption.

background subtraction for both runs is small in the signal interval $0^\circ-4^\circ$. The average level of the normalized background, plotted in larger angular intervals, is shown in fig. 4c as a dashed line histogram. The numbers of events ascribed to reaction (1) in the signal interval $0^\circ-4^\circ$, after subtraction of the normalized beam-gas background and the background from reactions (2), are given in table 1 for run I and II, respectively.

The cross section for reaction (1) can be written [15,16]

$$\begin{aligned} d\sigma(e^+e^- \rightarrow e^+e^-\eta) \\ = \frac{\alpha^2}{16\pi^4 E_b (E_b^2 - m_e^2)^{1/2}} \frac{d^3k'_1 d^3k'_2}{E'_1 E'_2} \frac{1}{q_1^2 q_2^2} \\ \times W_{TT} K_{TT}, \end{aligned} \quad (4)$$

where k'_1, E'_1 and k'_2, E'_2 are the three-momenta and energies of the scattered electrons, E_b is the beam energy and q_1 and q_2 are the four-vectors of the virtual photons. K_{TT} contains the density matrix elements for the transversely polarized, virtual photons and is given by formula (29d) in ref. [15]. The function W_{TT} is given by ^{#6}

^{#6} W_{TT} can also be expressed as [16] $2\sqrt{X} \cdot \sigma_{TT}$, where $X = (q_1 q_2)^2 - q_1^2 q_2^2$. In the limit $q_1^2 \rightarrow 0, q_2^2 \rightarrow 0, \sigma_{TT} \rightarrow \sigma_{\gamma\gamma}$, the cross section for two real photons forming an η . \sqrt{X} can then be interpreted as a flux factor.

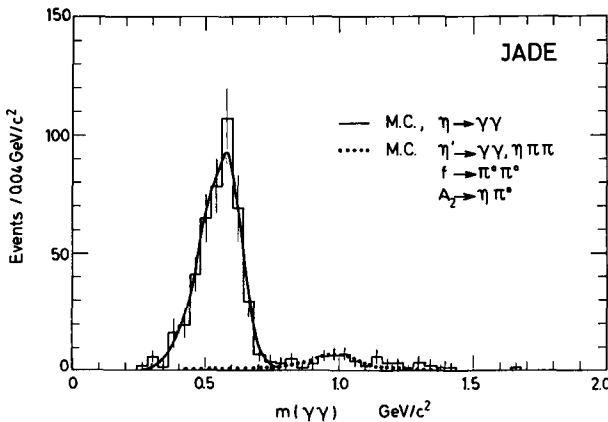


Fig. 5. Invariant $\gamma\gamma$ mass distribution for events of runs I and II selected with criteria (i)-(viii) for the angular interval $\Delta\phi = 0^\circ-4^\circ$, with beam-gas background subtracted. Data are shown with a continuous line histogram. The Monte Carlo simulation for reaction (1) and for reactions (2) are shown as a continuous curve and as a dotted curve, respectively.

$$\begin{aligned} W_{TT}(s, q_1^2, q_2^2) = \frac{1}{2} \pi (\nu^2 - m_\eta^2 Q^2) F_\eta^2(q_1^2, q_2^2) \\ \times \delta(s - m_\eta^2), \end{aligned} \quad (5)$$

where s is the squared $\gamma\gamma$ CM energy, $Q = \frac{1}{2}(q_1 - q_2)$ and $\nu = Q(q_1 + q_2)$. The factor containing ν and Q results from the coupling of the photons to the pseudoscalar η meson [17]. F_η is the η form-factor. Its q^2 -dependence was assumed to be that of a simple ρ -pole ^{#7}, i.e. F_η^2 is given by

$$\begin{aligned} F_\eta^2(q_1^2, q_2^2) = (\Gamma_{\eta \rightarrow \gamma\gamma} / 64\pi / m_\eta^3) (1 - q_1^2/m_\rho^2)^{-2} \\ \times (1 - q_2^2/m_\rho^2)^{-2}. \end{aligned} \quad (6)$$

The radiative width $\Gamma_{\eta \rightarrow \gamma\gamma}$ can be expressed as [18, 19]

$$\Gamma_{\eta \rightarrow \gamma\gamma} = \sigma(e^+e^- \rightarrow e^+e^-\eta) / I, \quad (7)$$

other angular limits in the integration changes $\Gamma_{\eta \rightarrow \gamma\gamma}$ by amounts which are smaller than the statistical precision of the Monte Carlo sample. Another systematic uncertainty stems from the assumed q^2 -dependence in (6), since the q^2 -dependence of the form-factor $F_\eta(q_1^2, q_2^2)$ is not known. Replacing the present assumption of the ρ -pole q^2 -dependence with a q^2 -dependence obtained by squaring the ρ -poles, or with the q^2 -dependence of a generalized VDM form-factor [20] changes $\Gamma_{\eta \rightarrow \gamma\gamma}$ by amounts smaller than or comparable with the statistical precision ($\sim(2-4)\%$) of the Monte Carlo samples. Thus we estimate that reasonable variations of the q^2 -dependence in (6) should cause less than a 5% change in the value of $\Gamma_{\eta \rightarrow \gamma\gamma}$.

Adding all of the above contributions in quadrature, we obtain a total systematic error of 8% and thus

$$\Gamma_{\eta \rightarrow \gamma\gamma} = 0.53 \pm 0.04 \pm 0.04 \text{ keV}.$$

The corresponding total width of the η meson is $\Gamma_\eta = 1.37 \pm 0.11 \pm 0.11 \text{ keV}$.

The η radiative width $\Gamma_{\eta \rightarrow \gamma\gamma}$ obtained in this experiment is inconsistent with the result reported by Browman et al. [10] of $\Gamma_{\eta \rightarrow \gamma\gamma} = 0.324 \pm 0.046 \text{ keV}$ at a significance level of $>99\%$ ($\sim 3\sigma$), and with the earlier result of Bemporad et al. [10] of 1.00 ± 0.22

^{#7} This assumption is motivated by the recent measurement of the q^2 -dependence of η' production in the reaction $e^+e^- \rightarrow e^+e^-\eta'$ [8].

keV at a significance level of 96% ($\sim 2\sigma$). Both of these experiments utilized the Primakoff effect in photoproduction and depend on the (theoretical) estimate of the nuclear electromagnetic form-factor and η production in the nuclear hadronic field. Our value is, however, in good agreement with the recent result of Weinstein et al. [12] of $0.56 \pm 0.12 \pm 0.10$ keV, which was also obtained in an e^+e^- storage ring experiment.

The $\gamma\gamma$ widths of the three neutral members of the pseudoscalar SU(3) nonet can be naively related as follows [21]:

$$\begin{aligned} \Gamma_{\eta \rightarrow \gamma\gamma} &= \frac{1}{3}(m_\eta/m_{\pi^0})^3 \\ &\times \Gamma_{\pi^0 \rightarrow \gamma\gamma}(\sqrt{8}r \sin \theta - \cos \theta)^2, \\ \Gamma_{\eta' \rightarrow \gamma\gamma} &= \frac{1}{3}(m_{\eta'}/m_{\pi^0})^3 \\ &\times \Gamma_{\pi^0 \rightarrow \gamma\gamma}(\sin \theta + \sqrt{8}r \cos \theta)^2. \end{aligned} \quad (8)$$

Here θ is the SU(3) octet-singlet mixing angle and r is the ratio of singlet and octet spatial wave functions at the origin. Using our value for $\Gamma_{\eta \rightarrow \gamma\gamma}$, the value $\Gamma_{\pi^0 \rightarrow \gamma\gamma} = 7.25 \pm 0.21$ eV^{*8} and the average value $\Gamma_{\eta' \rightarrow \gamma\gamma} = 4.42 \pm 0.34$ keV [14], we solve for r and θ and obtain

$$r = 0.96 \pm 0.03, \quad \theta = -18.4^\circ \pm 2.0^\circ.$$

This result is in good agreement with nonet symmetry ($r = 1$). The value of the mixing angle can be compared to the value from the quadratic mass formula [22], $\theta = -10^\circ$, or to a QCD calculation [23] giving $\theta = -17^\circ$ to -20° . In a study of the reaction $\pi^- p \rightarrow \eta' n$ [24], a value of $\theta = -16^\circ \pm 2^\circ$ was found.

We are indebted to the PETRA machine group and to the group of the DESY Computer Center for their excellent support during the experiment and to all engineers and technicians of the collaborating institutions who have participated in the maintenance of the apparatus. We express our thanks to F. Gutbrod and M. Poppe for helpful discussions. This experiment was supported by the Bundesministerium für Forschung und Technologie, by the Ministry of Education, Science and Culture of Japan, by the UK Science and Engineering Research Council through the Rutherford Appleton Laboratory and by the US Department of

Energy. The visiting groups at DESY wish to thank the DESY directorate for the hospitality extended to them.

References

- [1] S. Matsuda and S. Oneda, Phys. Rev. 187 (1969) 2107; S. Okubo, in: Symmetries and quark models, ed. R. Chand (Gordon and Breach, New York, 1970); A. Kotlewski et al., Phys. Rev. 8 (1973) 348; A. Bramon and M. Greco, Phys. Lett. 48B (1974) 137; F. Gault et al., Nuovo Cimento 24A (1974) 259; Etim-Etim and M. Greco, Nuovo Cimento 42 (1977) 124; V.M. Budnev and A.E. Kaloshim, Phys. Lett. 86B (1979) 351; S. Oneda and K. Terasaki, Supp. Prog. Theor. Phys., to be published.
- [2] H. Suura, T.F. Walsh and B.-L. Young, Lett. Nuovo Cimento 4 (1972) 505; M.S. Chanowitz, Phys. Rev. Lett. 15 (1975) 977; 44 (1980) 59.
- [3] J. Olsson, Proc. Vth Intern. Workshop on Photon-photon collisions (Aachen, 1983), Springer Lecture Notes in Physics, Vol. 191 (Springer, Berlin).
- [4] G. von Dardel et al., Phys. Lett. 4 (1963) 51; G. Bellettini et al., Nuovo Cimento 40A (1965) 1139; 66A (1970) 243; V.I. Kryshkin et al., JETP 30 (1970) 1037; A. Browman et al., Phys. Rev. Lett. 33 (1974) 1400; J.W. Cronin, Private communication.
- [5] D. Binnie et al., Phys. Lett. 83B (1979) 141; MARK II Collab., G. Abrams et al., Phys. Rev. Lett. 43 (1979) 477; CELLO Collab., H.J. Behrend et al., Phys. Lett. 114B (1982) 378; 125B (1983) 5 18(E);
- [6] JADE Collab., W. Bartel et al., Phys. Lett. 113B (1982) 190.
- [7] MARK II Collab., P. Jenni et al., Phys. Rev. D27 (1983) 1031.
- [8] PLUTO Collab., Ch. Berger et al., Phys. Lett. 142B (1984) 125.
- [9] TASSO Collab., M. Althoff et al., Phys. Lett. 147B (1984) 487.
- [10] C. Bemporad et al., Phys. Lett. 25B (1967) 380; A. Browman et al., Phys. Rev. Lett. 32 (1974) 1067.
- [11] H. Primakoff, Phys. Rev. 81 (1951) 899.
- [12] A. Weinstein et al., Phys. Rev. D28 (1983) 2896.
- [13] JADE Collab., W. Bartel et al., Phys. Lett. 88B (1979) 171; 92B (1980) 206; 99B (1981) 277.
- [14] A. Cordier, Proc. Vth Intern. Workshop on Photon-photon collisions (Lake Tahoe, USA, 1984).
- [15] G. Bonneau, M. Gourdin and F. Martin, Nucl. Phys. B54 (1973) 573.
- [16] V.M. Budnev et al., Phys. Rep. 15 (1975) 181.
- [17] G. Köpp, T.F. Walsh and P. Zerwas, Nucl. Phys. B70 (1974) 461.

*8 This value corresponds to $\tau_{\pi^0} = (0.897 \pm 0.022 \pm 0.014) \times 10^{-16}$ s (Cronin [4]).

- [18] S. Kawabata, Program Write-up (1982), unpublished; Contrib. parallel sessions, reported by J.H. Field, in: Proc. IVth Intern. Colloq. on Photon-photon interactions (Paris, 1981) p. 447.
- [19] H. Messel and D.F. Crawford, Electron-photon shower distribution function tables (Pergamon, London, 1970); A. Sato, Master's Thesis, Tokyo University (1978), unpublished.
- [20] I.F. Ginzburg and V.G. Serbo, Phys. Lett. 109B (1982) 231.
- [21] See, e.g., J.H. Field, Proc. Intern. Europhysics Conf. on High energy physics (Brighton, UK, 1983).
- [22] Particle Data Group, Rev. Mod. Phys. 56 (1984) 51.
- [23] A.T. Filippov, Sov. J. Nucl. Phys. 29 (1979) 534.
- [24] W.D. Apel, Sov. J. Nucl. Phys. 25 (1977) 300.